Original scientific paper

Informacije MIDEM
Journal of Microelectronics,
Electronic Components and Materials
Vol. 45, No. 4 (2015), 237 – 248

Angle of Arrival estimation algorithms using Received Signal Strength Indicator

Marko Malajner, Dušan Gleich, Peter Planinšič

University of Maribor, Faculty of Electrical Engineering and Computer Science, Maribor, Slovenia

Abstract: Angle of Arrival (AoA) is one of few techniques in the localization of a wireless sensor network. With two measured angles and with known distance between anchor the position of unknown node can be obtained. This paper deals with our approach of AoA measurement using a combination of more omnidirectional antennas on low-cost ZigBee modules which enable measurements of Received Strength Signal Indicator (RSSI). The used omnidirectional microstrip antenna has almost a symmetrical radiation pattern with sharp minimums along the x antenna axis. Therefore, an algorithm based on an approach where an angle of arrival is obtained along a direction where the measured RSSI is minimal. This paper presents on our approach proposed methods, algorithms and comparison of them.

Keywords: Angle of Arrival, Localization, Wireless Sensor Networks, RSSI

Algoritmi za ocenjevanje kota prihoda RF signala z uporabo indikatorja moči

Izvleček: Kot prihoda signala je ena izmed lokalizacijskih tehnik, ki se uporabljajo v brezžičnih senzorskih omrežjih. Z dvema izmerjenima kotoma in z znano razdaljo med dvema svetilnikoma lahko določimo pozicijo neznanega vozlišča. V tem članku bomo opisali naš princip ocenjevanja kota prihoda s pomočjo kombinacije večih neusmerjenih anten. Uporabili smo cenovno ugodne ZigBee module, ki omogočajo merjenje sprejete moči signala ter iz tega izluščili kot prihoda. Antena, vgrajena na modulih, je praktično neusmerjena, z dokaj simetričnim sevalnim diagramom, z dvema ostrima robovoma vzdolž x osi antene. Kot prihoda signala je v smeri, v kateri smo izmerili minimalne vrednosti sprejete moči. V tem članku bomo opisali nekaj različnih metod in pripadajočih algoritmov, ki smo jih razvili ter naredili primerjavo.

Ključne besede: Kot prihoda RF signala, Lokalizacija, Brezžična senzorska omrežja, RSSI

* *Corresponding Author's e-mail: marko.malajner@um.si*

1 Introduction

Localization is a crucial mechanism for obtaining the locations of data source or sink within wireless sensor networks (WSN). WSN consists of small so-called wireless sensor-nodes (further simple denoted as sensors or nodes), equipped with environmental sensing devices, power sources, radio and processor units. Sensors can communicate with each other or with the base–station. In many cases the sensors are randomly deployed on fields where locations information not exist in advance. Some localization systems must be performed on sensors' fields for locating each sensor.

Two physical values are primarily measured, separately or in combination, when positioning wireless sensor nodes: (i) time of radio frequency (RF) signal flight (ToF) and (ii) the power of the received RF signal. The distances or angles between the nodes are then calculated (via trilateration or triangulation) [20] from these primary values for determining the locations of each node. Three main localization techniques are known in WSN: (i)ToF – Time of Flight, (ii) RSSI – Received Signal Strength Indicator and (iii) AoA – Angle of Arrival [1, 22]. Measuring the ToF is costly because the RF signal propagation has the speed of light and therefore the nodes must have a common accurate clock, or exchange of timing information using certain protocols as, for example, a two-way ranging protocol [2, 3]. Most 802.11 and 802.15.4 radio modules support the measuring of RSSI, which enables the calculations of received power for each received packet [6]. The power or energy distribution of a RF signal traveling between two nodes is

a signal parameter which can be used for distance estimation, depending on the path-loss and shadowing effects. RSSI measurements are very uncertain because there are several disturbing sources like many delayed multipath signals arriving at the receiver [4, 5]. AoA or directions to neighboring sensors can be estimated from ToF and/or RSSI. There are two common ways how sensors measure the AoA, i) multiple static smart antennas or arrays and ii) rotatable antennas.

Localization systems using multiple static antennas or arrays for AoA-measurements. Usually they are called smart antennas, because they use signal processing units for AoA measurements. The most common method is to use antenna array with known array geometry, and measuring the differences of signal arrival times at different antennas [7]. Authors in [8] estimates AoA at each receiving node via frequency measurement of the local RSSI. Another method uses antenna arrays and RSSI measurements on each antenna and from their RSSI -ratios the AoA can be estimated [9, 10, 11]. On the other hand AoA systems can uses beamforming [12, 13]. Beamforming on static antennas system can shape radiation pattern without physical shaping of antennas. This can be done with switching each individual antenna "on" or "off" with various algorithms. Adaptive smart antennas are the second category of antennas where adaptive beam is formed based on the direction of the desired and interfering sources [13]. In [14] authors proposed AoA estimation based on subarray beamforming. The target AoA is estimated from the phase shift introduced in the target signal by subarray beamforming. In the literature many algorithm can be found for estimating AoA from antennas arrays or smart antenna, such are MUSIC [15], root MUSIC [16], maximum likelihood estimator [17], ESPIRIT [18], etc.

Many AoA techniques using rotatable antennas with shaped radiation patterns in one direction and then seek the maximal power of the received signals around the axis [19, 21].

This paper presents our proposed methods of AoA estimation using a system of multiple omnidirectional monopole static and rotatable antennas placed on the circumference of a circular plate. The radiation shape of the used monopole antenna is not ideally isotropic and has a tiny minimum in the direction of the antenna axis. The idea presented in this paper is to find from which direction the minimal RSSI is measured. Searching for the minimum was chosen because better selectivity is obtained due to the tiny sharp minimum within the radiation pattern of the antennas system. Rotatable antennas have advantage because of better resolution on the other hand the advantage of a static plate is that all movable parts are eliminated. We also show that the static system has a slightly lower resolution, but can be improved by interpolation or approximation

The rest of the paper is organized as follow: Section II provides the theoretical background, Section III presents the used hardware, Section IV presents the experimental verification of the proposed method with rotatable antennas, Section V shows the experimental verification of the proposed method with static antennas, Section VI compares the used methods, and Section VII concludes the paper.

2 Theoretical background of our approach

The dipole antenna is considered as an omnidirectional antenna. The ideal dipole has a spherical radiation pattern, which radiates isotropically. A real dipole has some degree of directivity and radiates weaker in the direction of the antenna axis. The performance of a linearly-polarized antenna, which is almost an approximation of an ideal antenna, is described with *E*– and *H*–plane patterns [23]. The *H* [A/m]– and *E* [V/m]– planes are perpendicular to each other. The cross–product of *E* and *H** (* denotes complex conjugation) divided by 2, gives the time-average Poynting vector of the radiated field.

The orientation of used short dipole antenna is shown in Figure 1. and the radiation pattern of antenna can be expressed as approximation of triangular current distribution in spherical coordinates:

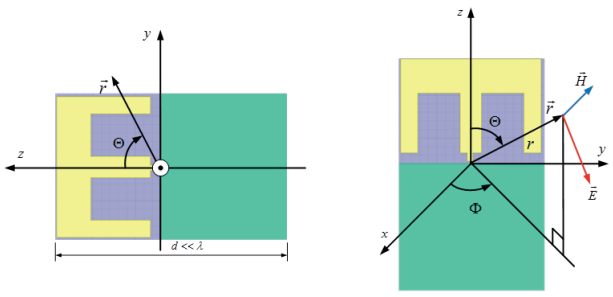

Figure 1: Orientation of antenna in coordinate system

$$\vec{E} \approx \vec{1}_{\Theta} \frac{jkZ_0}{8\pi} I_g l \frac{e^{-jkr}}{r} \sin\Theta \tag{1}$$

$$\vec{H} \approx \vec{1}_{\Theta} \frac{jk}{8\pi} I_g l \frac{e^{-jkr}}{r} \sin\Theta \tag{2}$$

where $k = \omega\sqrt{\mu_0\varepsilon_0} = 2\pi/\lambda$, $Z_0 = \sqrt{\mu_0/\varepsilon_0}$, r is the length of spherical vector $\vec{r} = (r, \Theta, \Phi)$, Θ is the azimuth angle, and F is the latitude angle. I_g is a source

current and *d* is the length of antenna. The 2–D omnidirectional radiation patterns are presented in Figure 2, obtained by Ansoft HFSS [25]. It is simulation of antenna, used in our experiments.

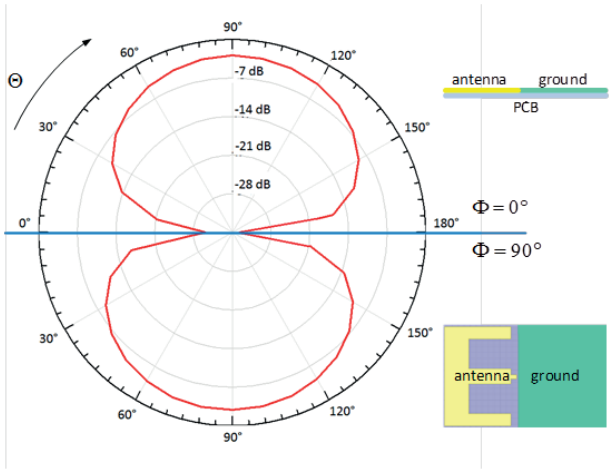

Figure 2: E-plane radiation of used antenna.

It can be observed from the radiation pattern in Figure 2 that the pattern has all the characteristics of short dipole. On the right side in Figure 2 it is orientation of the used antenna in respect to the radiation pattern. The radiation pattern in Figure 2 consists of two zones of tiny decreased intensity at 0 and 180 degrees. The RF signal, which arrives from the transmitter in the direction where radiation pattern has less sensibility, causes lower RSSI. For analytically searching angle Θ with minimum radiation value we should solve the following equation:

$$F\left(\Theta,\Phi\right)=0 \tag{3}$$

We can see that the analytically minimums of the simplified radiation pattern of dipole appear at every 180. Real dipole has a little difference between two minimums as is shown in Figure 2 and Figure 3. This difference is about a few dBs and can be detected with algorithm. Therefore, the minimums of real dipole appear at integer multiple of 2π i.e. $\theta = k \cdot 2\pi;\ \mathrm{k} \in Z.$

In this paper, two different methods using our proposed approach are presented and compared. i) system with 4 rotatable antennas, partly presented in [4], ii) system with 12 static antennas which uses approximations and interpolations for AoA obtaining, partly presented in [26].

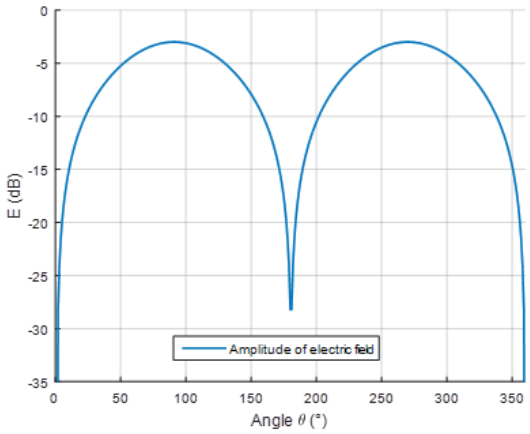

Figure 3: Radiation pattern of single antenna

3 Hardware set-up

The device for the proposed AoA measurement in our case consists of transceivers (used as receivers) placed on a circular plate. The plate with transceivers MRF24J-40MA is attached to our SPaRCMosquito WSN board with a Cortex M3 NXP microcontroller, and a battery-powered source. The transceivers use microstrip antenna operating within the ISM 2.4 GHz band. Monopole antenna uses ground plane of MRF24J40MA module and ground plane of circular plate as a counterpoise ground plane. Additional ground plane on our circular plate enhance the performance of module [27] and does not significantly reshape the radiation pattern.

In this section two types of proposed hardware are presented. First is rotatable and consists of 4 antennas and second is static (without mechanical moving parts) with 12 antennas.

3.1 Rotatable antennas

First version of receiving device for AoA measurement consists of a four transceivers placed on circular plate (Fig. 4a), a stepper motor (Fig. 4c), a driver circuit for stepper-motor (Fig. 4d), a WSN board-1 for controlling the receiver plate (Fig. 4b), and WSN board-2 for communication with computer (Fig. 4e). A 200 steps-per-revolution motor is used to rotate the plate with transceivers. The stepper motor-driver is the well-known integrated circuit L298. The plate with four transceivers is attached on the WSN board-1. The entire device for measuring AoA, including power-source, is mounted on the axis of stepper motor. The slipping rings for communications and power supply are eliminated because of this. WSN board-2 is also provided for controlling the stepper-motor.

During the experiments, the stepper motor turns the plate using receivers with resolutions of 3,6°. The transmitter (Fig. 4f) continually transmits RF signal. For each position of the plate, the receivers measure RSSI and then the data is sent to board-1, which wireless communicates with WSN board-2. The transmitter transmits about 40 packets of data at each position of stepper motor. WSN board-2 is connected via USB to laptop where the data is collected and later processed to estimate AoA.

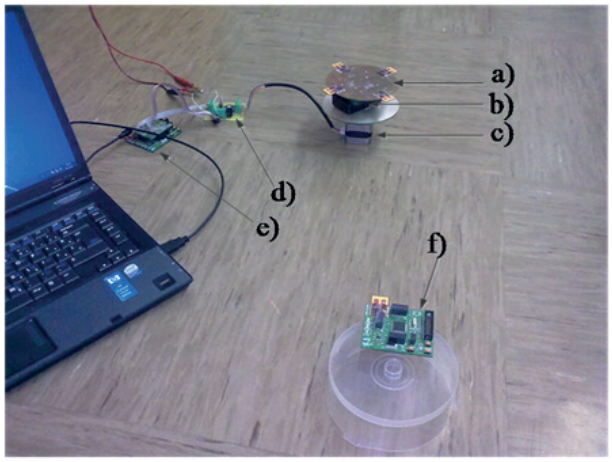

Figure 4: The rotatable AoA measuring experimental set-up.

3.2 Static antennas

We decided to build simplest static version of hardware in order to eliminate mechanical moving parts witch are not practical in real use of the device. Instead of stepper motor we added more antennas on circle plate and try to achieve the same effect, as with four rotatable antennas. Static measurement device is shown in Figure 5.

The measurement proceeding is next: The transmitter (Figure 5c) continually transmits RF signals during the experiments. The SPaRCMosquito boards (Figure 5b) with receivers on circular plate (Figure 5a) collects the RSSI values from each receiver. Approximately 40 packets of RSSI data are collected and averaged. Each transmitted packet was received on all receivers simultaneously. The averaged RSSI data were then sent to the laptop for further processing.

4 Description and experimental verification of the proposed method with rotatable antennas

The presence of a moving object or humans in the vicinities of the transceivers causes large fluctuations in the RSSI measurements, therefore all the experiments were carried-out within environments without obstacles and moving objects, and in the line of sight (LOS). The experiments were conducted within both indoor and outdoor environments for different distances between transceivers.

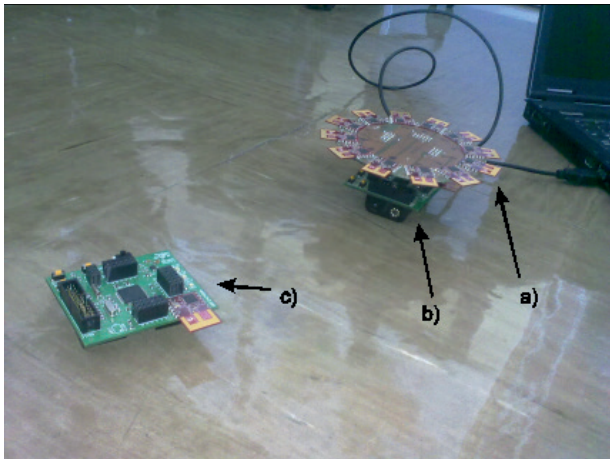

Figure 5: Static AoA measuring system. a) Plate with transceivers. b) Main measurement control device – SPaRCMosquito. c) SPaRCMosquito as a transmitter.

4.1 Algorithm for AoA estimation method with rotatable multiple antennas

The goal of the algorithm is to find the AoA where minimums of RSSI appear. The simple algorithm for gathering the RSSI from each receiver is as follows. Firstly, the transmitter sends one packet with dummy data. All transceivers on the circular plate are in receiving mode and waiting for incoming packet. When the receivers receive a packet, they calculate the RSSI from the voltage of the incoming RF signal. One of receivers is connected to a microcontroller interrupt line. When receiver sends an interrupt to microcontroller, the reading phases are started. The microcontroller via SPI reads the RSSI data from each receiver in a sequence. When the reading is done, the command for next step is sent. This procedure is repeated until complete revolution of motor is done. All readings are sent to PC for further processing. On PC, specially developed software is gathering this data in files. In this files are saved RSSI readings of each antenna together with information of position of motor. This files serves as input for the Matlab algorithm for AoA estimation by analyzing t RSSI data. Simple algorithm first shifts obtained RSSI curves of antennas and then searches for the minimums of averaged curves. Where the global minimum appears, there algorithm reads the corresponding angle and adds ± 180° and estimated AoA. Figure 6 show principle of proposed method.

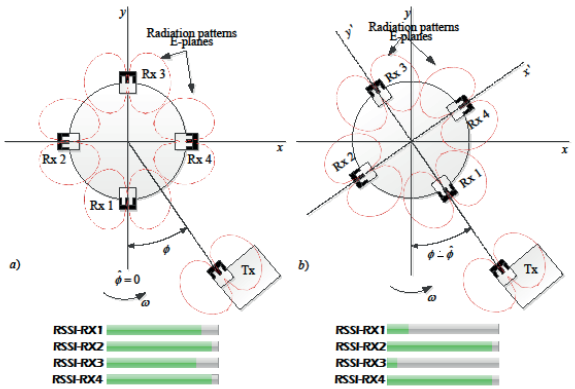

Figure 6: Top view of measuring device, and the coordinate system for measuring AoA. a) Initial set-up with unknown position of transmitter (Tx), bar graphs show measured RSSI-values. b) The scenario where the true AoA is obtained. The minimums of measured RSS-valuesl on Rx1 and Rx3 can be observed on the bar graphs.

4.1.1 Outdoor experiments

Outdoor experiments were carried-out on an asphalt floor in a line–of–sight between transceivers. The transceivers were placed at a 1m height from ground, on a rack. The true AoA was set at 54. Figure 7 shows the measured RSSI versus rotating-angle at a distance between the transmitter and the receiver of 2 m.

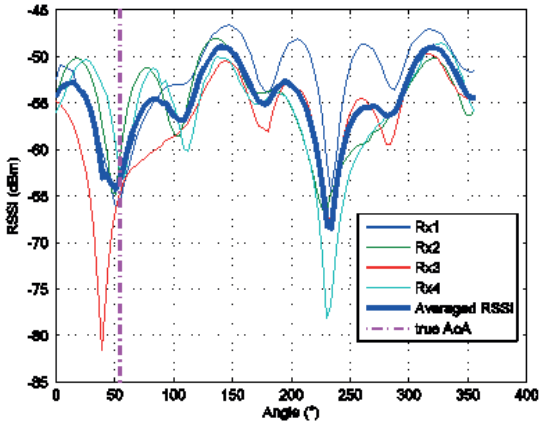

Figure 7: Shifted and averaged RSSI vs. angle at distance 2m outdoor.

In some cases measurements are corrupted because of reflection from ground and other obstacles.

4.1.2 Indoor experiments

Indoor experiments were carried-out in LOS in a 6 m-by-8 m room in LOS between transceivers; the true angle was set at 54°. The transceivers were placed at 1 m in height. The experiments were carried-out in the same way as the outdoor experiments. Figure 8 shows received RSSI from all antennas versus angle. The indoor measurements were influenced by reflected signals from the walls, floor, ceiling, furniture, and other objects. Therefore, the RSSI curves were not as smooth, having more local minimums and maximums, and it was more difficult to accurately estimate the AoA than during outdoor measurements. These effects are extremely visible in Figure 9 where we can observe lot of minimums and the algorithm therefore fails to obtain correct AoA.

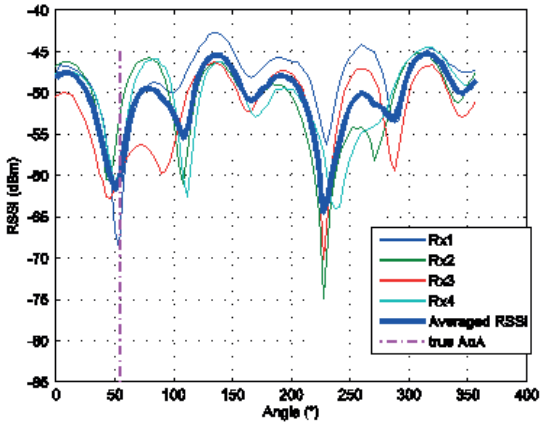

Figure 8: Shifted and averaged RSSI vs. angle at distance 3m indoor.

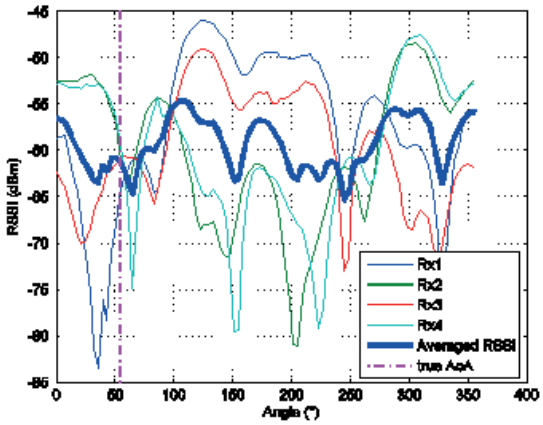

Figure 9: Shifted and averaged RSSI vs. angle at distance 5m indoor.

4.1 Outdoor and indoor accuracies

The transmitter was placed at distances from 1 m to 6 m, with steps of 1 m. All measurements were repeated 3 times at same position of transceivers. Figure 10 shows the averaged errors between estimated and true AoA for three complete estimation procedures at different distances in outdoor environment. The maximum absolute mean error of the estimated AoA was about 4°.

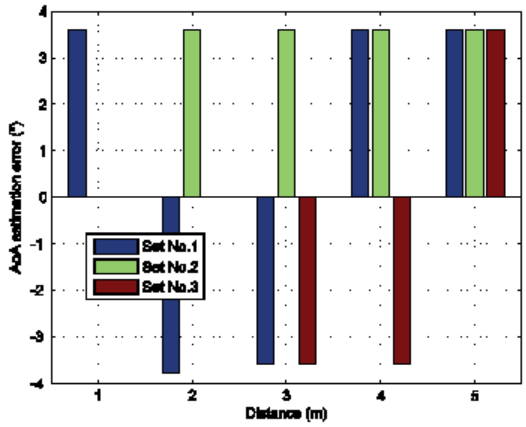

Figure 10: The error of the estimated AoA from all outdoor tests as a function of the distance between transmitter and receiver.

Fig. 11 shows the errors between the estimated and true AoA over different distances for indoor environment. The angle was estimated three times using the complete proposed algorithm. The maximum absolute mean error was about 8°.

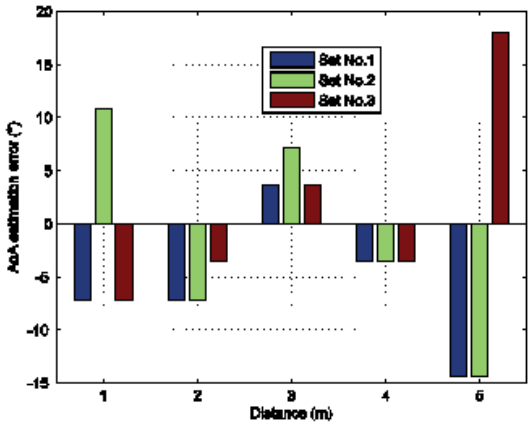

Figure 11: The errors of estimated AoA from all indoor tests as a function of the distance between transmitter and receiver.

5. Description and experimental verification of the proposed method with static antennas

5.1 Simple algorithm for AoA estimation with multiple static antennas

The radiation pattern of monopole is well-known and can be calculated from equations (1) and (2). With the proposed antenna arrangement, twelve static dipole patterns placed around the circle can be imagined. Figure 12 shows only 4 of 12 antenna's patterns (E–planes) because of transparency.

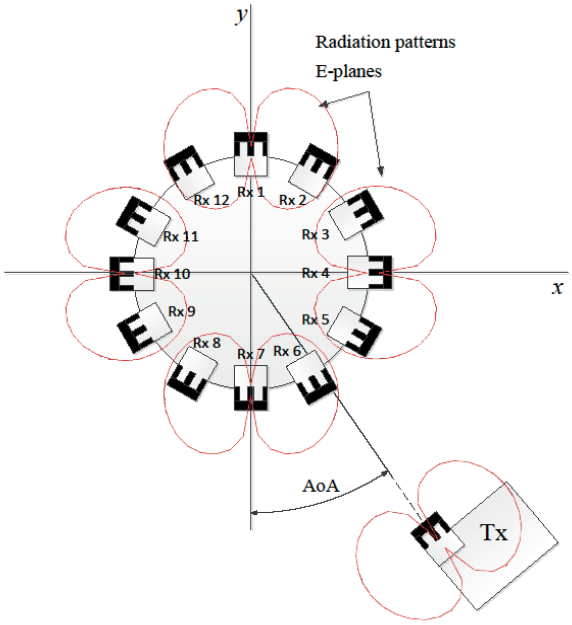

Figure 12: Principle of AoA measuring system with multiple static antennas.

The simple algorithm for gathering the RSSI-values from each receiver is as follows. Firstly, the transmitter sends one packet with dummy data. All the transceivers on the circular plate are in receiving mode and waiting for incoming packet. When the receivers receive a packet, they calculate the RSSI from the voltage of the incoming RF signal. One of receivers is connected to a microcontroller interrupt line. When the receiver sends an interrupt to the microcontroller, the reading phases starts. The microcontroller via SPI reads the RSSI data from each receiver in a sequence. When the reading is done, the transmitter sends a new data packet. RSSI measuring is repeated till 40 packets are processed and averaged. The on–line phase of the algorithm is finished with the last operation.

The off–line part of algorithm is performed on a laptop. Special software was developed only for gathering data from the measuring device via USB to the laptop. The software writes the averaged RSSI of each receiver in the file, including the receiver's number. This file serves as input for the Matlab algorithm for AoA estimation by analyzing RSSI -data. Basically, simple algorithm searches for receiver, at which minimum of RSSI data is measured. The true AoA is in the opposite direction ($\pm$ 180°) of minima. By this proposed method, the reso- lution of AoA is 360°divided by the number of receivers, in our case 30°, because the antennas are equally arranged around the circle.

5.2 Experimental estimations of AoA using simple algorithm

All experiments were carried-out within a real environment, outdoor and indoor. Measurements were limited to line of sight (LOS) between transmitter and receivers. Moving and static obstacles caused significant fluctuations in the measurements of the received power. Each experimental set-up was repeated three times and the results averaged.

5.2.1 Outdoor experiments

Outdoor experiments were carried-out on an asphalt floor with line-of-sight between transceivers. The transceivers were placed on a rack at 1m height from the ground. The transmitter was placed at distances from 1m to 30 m, at steps of 1 m. Figure 13 shows the measured RSSI points versus angle at a distance between the transmitter and the receiver of 1 m. In first case, the true azimuth AoA was set at 90°. The algorithm searches for angle with measured minimal RSSI-value, which was in this case at 270° i.e. at the 9rd antenna. The estimated AoA was 270°-180°= 90°and completely matched the true AoA, set in advance.

In the second case the true AoA was set between antennas 3 and 4. The RSSI measurements are shown in Figure 14. By algorithm estimated AoA was again at 90°, and the true AoA was set at 105°. The estimation error in this case was about 15°and was a consequence of the fixed resolution of this proposed method, in our case 30°, as mentioned in previous section.

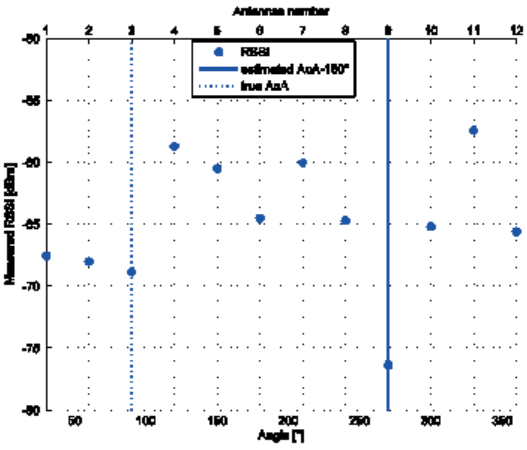

Figure 13: Outdoor measurements of RSSI versus angle at a distance of 1 m.

5.2.2 Indoor measurements

Indoor measurements were carried-out in a 6 m-by-8 m room and in underground garage. The transceivers were placed at 1m heights. The experiments were carried-out in the same way as the outdoor experiments.

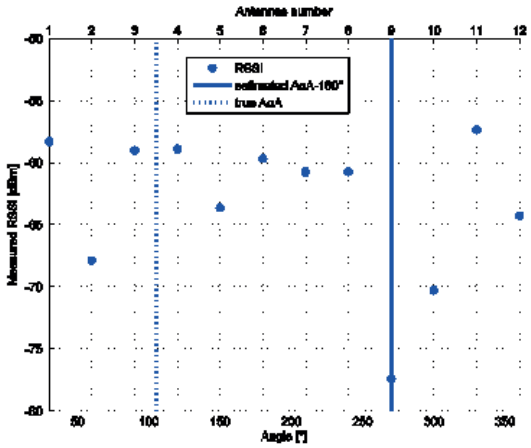

Figure 14: Outdoor measurements of RSSI versus angle at a distance of 3 m and true AoA at 105°.

Figure 15 shows the measured RSSI versus azimuth angle. The measurements were done at a distance of 1m and an angle of 90°. The indoor measurements were influenced by the reflected signals from the obstacles in the room. Due to reflected signals, the RSSI measurements contained more local minimums and maximums and it was more difficult to accurately estimate the AoA than during outdoor measurements and therefore the differences between local minimums were smaller. However, despite small differences s, the AoA estimation was very close to the true value. In the case depicted in Figure 15, the algorithm found the smallest RSSI at the 9rd antenna (270°-180°), where also the true AoA of 90° was set.

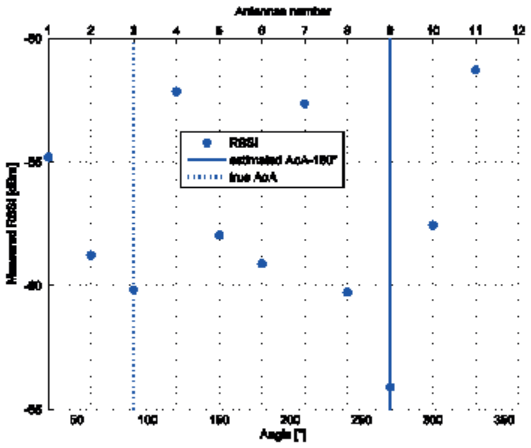

Figure 15: Indoor measurements of RSSI versus angle at 1m

Figure 16 shows the case where the true AoA was set at 105°and the distance between the transceivers was 3 m. The algorithm estimated AoA at 300°-180°, where the smallest RSSI was measured. The greater errors during indoor estimation were the consequences of unconsidered reflective signals from the obstacles. Due to the disturbing reflections from the obstacles, the esti-

mation errors in indoor environment were, in general, greater than a resolution of 30°.

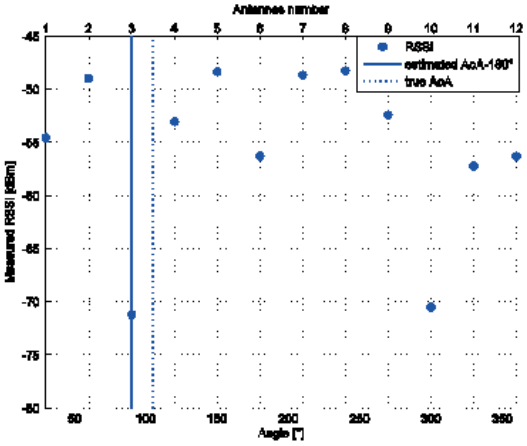

Figure 16: Indoor measurements of RSSI versus angle at 5 m. True AoA was at 105°

5.3 Improved AoA- estimation algorithm

The interpolations and approximations between RSSI points were realized in order to improve the resolution and accuracy of the simple algorithm of AoA method, and then the angle, by witch minimum on curve with interpolated RSSI-values was searched for. Different interpolations and approximations were used and compared. In this subsection all the experiments were taken outdoors at distances of 2 meters.

5.3.1 Linear and spline interpolations

The simplest is interpolation which connects points with lines. However, this interpolation does not improve the accuracy of AoA estimation by searching the minimum. The next interpolation is cubic spline. Spline interpolation uses low-degree polynomials at each of the intervals, and chooses the polynomial pieces so that they fit smoothly together. Figure 17 shows the linear and spline interpolations where the true AoA was at 90° and in Figure 18 where the true AoA was at 105°. Where the true AoA was set in the direction of antenna 3, both the linear and spline interpolations gave the same minima of close to 90°. Figure 18 depicts a case where the true AoA was between antenna 3 and 4 (105°). Using linear polarization, the algorithm returned AoA at 90°, which meant the error was about 15°. The algorithm with spline polarization estimated AoA at 99°and the error was much lower, at about 6°.

5.3.2 Polynomial and Gaussian approximations

In this case the Polynomial and Gaussian approximations were included in the algorithm. When the number of data points (in our case twelve) is equal to an order of degree of polynomial, then interpolation is

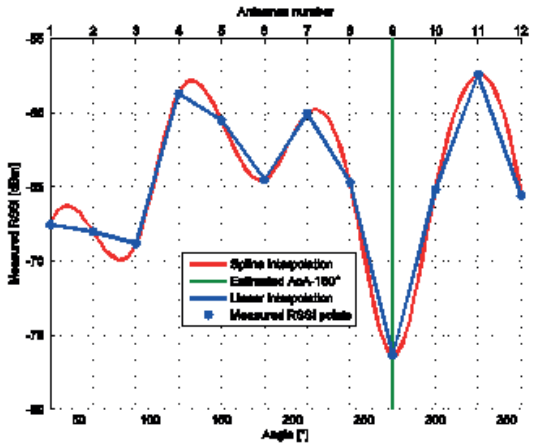

Figure 17: Outdoor measurement using linear and spline interpolation (distance 2 m).

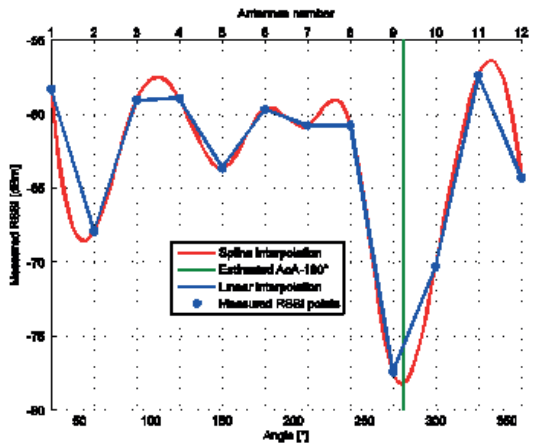

Figure 18: Outdoor measurement using linear and spline interpolation at true AoA at 105°

obtained and the polynomial goes through all the data points. The Gaussian process is a powerful non-linear interpolation tool. In addition the Gaussian function, it can not only be used for fitting an interpolant that passes exactly through the given data points but also for regression, i.e., for fitting a curve through noisy data [28].

A curve–fitting tool by Matlab [29] was used for calculating the polynomial coefficients. Fig. 19 shows the approximated data with polynomial of the 9th degree:

$$y(x) = p_1 \cdot x^9 + p_2 \cdot x^8 + \ldots p_8 \cdot x^2 + p_9 \cdot x + p_{10} \quad (4)$$

The algorithm with polynomial approximation returned 91°, the estimated AoA was a little closer in comparison to linear polarization. The error was about 14°.

Gaussian approximation used general model Gauss2 with equation:

$$y(x) = a_1 \cdot e^{(-((x-b_1)/c_1)^2)} + a_2 \cdot e^{(-((x-b_2)/c_2)^2)} \quad (5)$$

The result of Gaussian approximation is in Fig. 20. The estimated AoA was almost exactly at 105°, with an error of 0°. In this case the Gaussian approximation was the best choice.

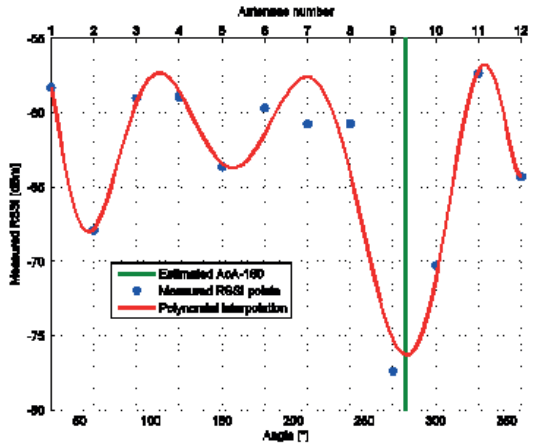

Figure 19: Outdoor measurement using polynomial approximation using 9th degree polynomial (distance 2 m).

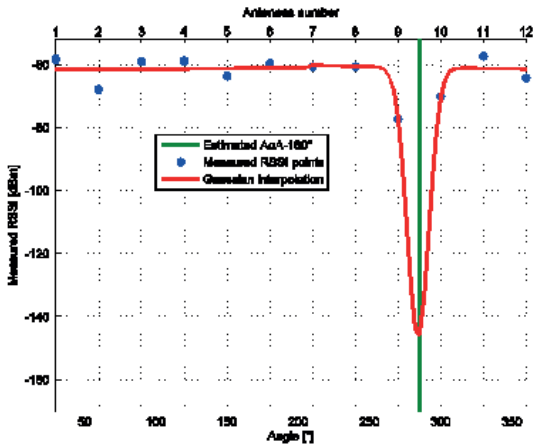

Figure 20: Outdoor measurement using Gaussian approximation at true AoA at 105°.

5.3.3 MUSIC estimator

In regard to comparisons between interpolations techniques we implemented the MUSIC (Multiple Signal Classification) estimator [13] for obtaining AoA. This MUSIC algorithm is well–known in AoA estimation. The inputs of the MUSIC algorithm are usually the amplitude and phase of the received signal. MRF24J40 radio modules return just the amplitude of a signal (RSSI). The authors in [13] (Chapter 10, p.343) reported a MUSIC estimator which neglected information about the signal phase. This RSSI estimator is defined as follow:

The RSSI value on each i-th antenna can be written as:

$$S_i[k] = G_i(\theta)x_i[k] + n_i[k]; \quad (6)$$

where $G_i(\theta)$ are the gains of each antenna, $x_i[k]$ are those signals assumed as being non–correlated from snapshot to snapshot *[k]*. An estimation of the correlation matrix R_{ss} of the received signal is:

$$\hat{R}_{ss} = \frac{1}{K}\sum_{k=i}^{K} S[k]S[k]^T \quad (7)$$

By applying the single-value decomposition, a set of three following matrices is obtained:

$$\hat{R}_{ss} = USU^* \quad (8)$$

The space spanned by the signal is partitioned as $U = [U_s, U_n]$, where the matrix U_s contains the singular vectors corresponding to the largest singular value, and the matrix U_n containing the singular vector corresponding to the smallest singular values. U_s is signal subspace, and Un is signal null space (complementary space of the signal subspace). Because *U* is a unitary matrix, the signal and noise subspaces are orthogonal, (<*Us,Un* >= 0). This can be defined as a pseudo-spectrum of the MUSIC algorithm:

$$P_{MUSIC}(\theta) = \frac{1}{G(\theta)U_n}, \quad (9)$$

which exhibits a peak of angle (θ) close to the actual angle ($\hat{\theta}$).

Basically the RSSI MUSIC estimator searches areas where the maximums in the signals appear. In our case it is necessary to search for the minimums of the received signal and because of that we arranged an input signal for the MUSIC estimator. The raw measured signal depicted with dots in Fig. 21 is mirrored (depicted in Fig. 20) before going to the MUSIC estimator. The mirrored signal exhibits peaks instead of minimums which are crucial for correct MUSIC estimation. In regard to this modification, the parameters of the MUSIC estimator must be set appropriately. Instead of the beam width of the antenna, we used the width of the so–called 'cone of silence' which is the opposite of the beam width, in our case 20°. Fig. 20 shows the measured mirrored signal and the pseudospectrum of a signal as an output of the MUSIC estimator. The amplitudes of both signals are adjusted for better representation in Fig. 20.

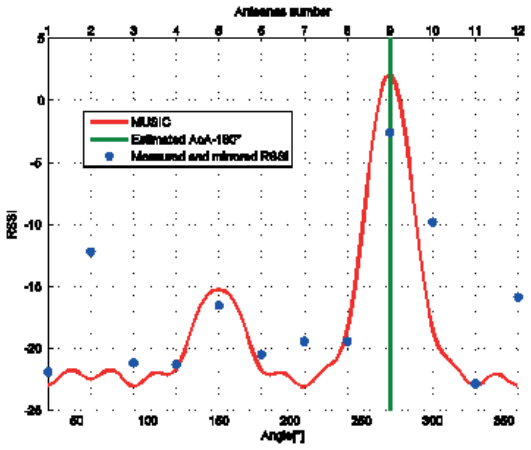

Figure 21: MUSIC estimator used on mirrored RSSI measurements.

5.4 Comparison of improved algorithms accuracies with different interpolations/ approximations

The interpolations improved the accuracy of AoA estimation using, in our case, multiple static omnidirectional antennas. The resolution of the estimation was 30° using the simple algorithm without interpolations and approximations. This section provides the comparison of results between algorithms by used the different interpolations/approximations.

Fig. 22 shows AoA estimation using five interpolations at a few different pre-set AoA's. Measurements were carried-out outside in LOS between transceivers. The linear interpolations provided an average error of about 15°. Polynomial approximation was slightly better and returned about 10° of error. The MUSIC estimator returns similar results on average as polynomial approximation. Much more accurate were the Spline and Gaussian interpolations/approximations where the errors reached about 6° and 4°, respectively.

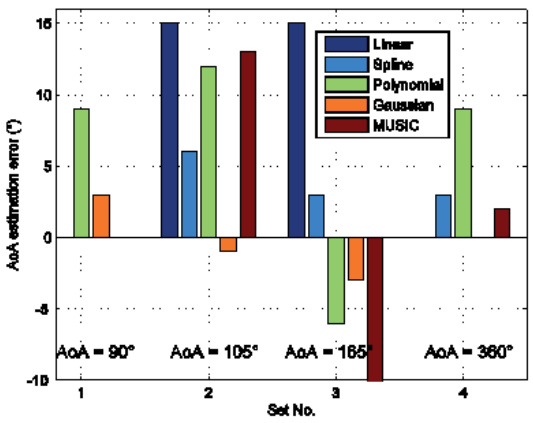

Figure 22: Outdoor deviations at different pre-set AoA's (distance 2 m).

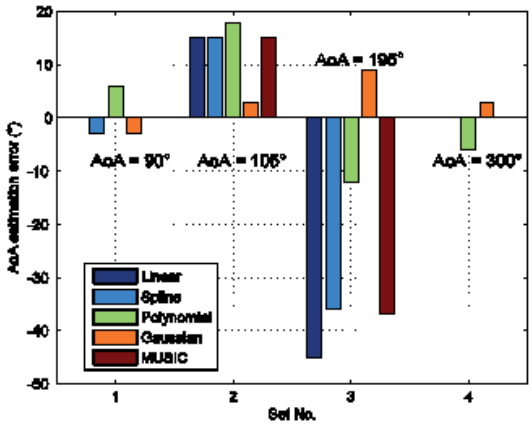

Figure 23: Indoor deviations at distance of 1 m.

The indoor measurements were more problematic because of the influences of reflected signals from the obstacles. Meanwhile, because LOS were between the transceivers, large fluctuations were caused by reflected signals from the floor, ceiling, walls, furniture, etc. Reflections of the signal causes "fake" minimas, which cannot be very successfully eliminated by our improved algorithm. Therefore the errors of AoA estimates were larger within the indoor environment. Again, Fig. 23 shows that the best results were obtained using Gaussian -approximation at all AoA measurement points.

6 Comparison of accuracies using rotatable and static antennas

The last Fig. 24 shows an overall comparisons between all the different interpolation/approximation methods and with different hardware within different environments. It was expected that the bigger errors would be within the indoor environment. The errors from all measurements at all distances were averaged and presented in % of 360° for each method. Rotatable antennas gave the best AoA estimation because of higher resolution in comparison with static antennas. Relative errors were about 5% for outdoor and 14% for indoor measurements. On the other hand static antennas and Gaussian approximation provided the best results, with outdoor errors of about 3% and indoor about 18%, respectively. The spline and Linear interpolations and MUSIC estimator returned approximately similar results. The maximum errors were obtained by Polynomial approximation because of oscillations. The results show, that the Gaussian approximation improved the accuracy of AoA estimation within static antennas.

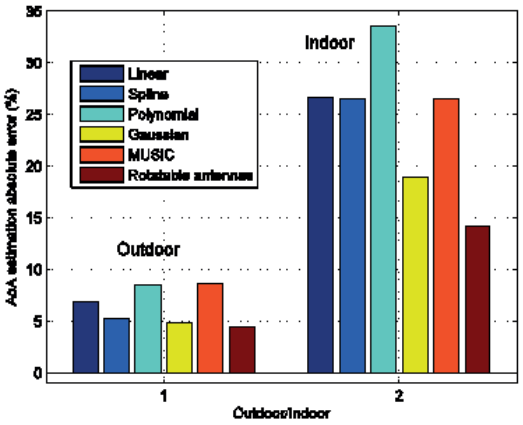

Figure 24: Comparison of all proposed methods.

7 Conclusions

In this paper we compared accuracies of two AoA estimations method. First method based on rotatable multiple antennas and second based on multiple static antennas. Rotatable antennas has resolution 3,6° and static antennas has resolution 30°. We showed that it is possible to improve accuracy of static antennas with interpolations/approximations. Hoverer, rotatable antennas gave the best results than static antennas with improved algorithm. But static antennas has advantage because all movable parts are eliminated. Overall comparison of result shows that the best results gave rotatable antennas (about 4% outdoor and 14% indoor relative error), close to this results gave static antennas and Gaussian interpolation (about 5% outdoor and 18% indoor error).

8 References

1. L. Bras, N.B. Carvalho, and P. Pinho. Pentagonal patch-excited sectorized antenna for localization systems. Antennas and Propagation, IEEE Transactions on, 60(3):1634–1638, 2012. doi:10.1109/TAP.2011.2180339.
2. N. Patwari, A.O. Hero, M. Perkins, N.S. Correal, and R.J. O'Dea. Relative location estimation in wireless sensor networks. Signal Processing, IEEE Transactions on, 51(8):2137–2148, 2003. doi:10.1109/TSP.2003.814469.
3. S. M. Lanzisera. RF Ranging for Location Awareness. PhD thesis, UC Berkeley, 2009.
4. M. Malajner, K. Benkic, P. Planinsic, and Z. Cucej. The accuracy of propagation models for distance measurement between wsn nodes. In Systems, Signals and Image Processing, 2009. IWSSIP 2009. 16th International Conference on, pages 1–4, 2009. doi:10.1109/IWSSIP.2009.5367782.
5. N. Patwari, J.N. Ash, S. Kyperountas, A.O. Hero, R.L. Moses, and N.S. Correal. Locating the nodes: cooperative localization in wireless sensor networks. Signal Processing Magazine, IEEE, 22(4):54–69, 2005. doi:10.1109/MSP.2005.1458287.
6. M. Botta, M. Simek Adaptive Distance Estimation Based on RSSI in 802.15.4 Network RADIOENGINEERING,, VOL. 22, NO. 4, December 2013 .
7. S. Maddio, A. Cidronali, and G. Manes. An azimuth of arrival detector based on a compact complementary antenna system. In Microwave Conference (EuMC), 2010 European, pages 1726–1729, 2010.
8. Weile Zhang, Qinye Yin, Hongyang Chen, Feifei Gao, and N. Ansari. Distributed angle estimation for localization in wireless sensor networks. Wireless Communications, IEEE Transactions on, 12(2):527–537, 2013. doi:10.1109/TWC.2012.121412.111346.
9. M. Abusultan, S. Harkness, B.J. LaMeres, and Yikun Huang. Fpga implementation of a bartlett direction of arrival algorithm for a 5.8ghz circular antenna array. In Aerospace Conference, 2010 IEEE, pages 1–10, 2010.
10. M.R. Kamarudin, Y.I. Nechayev, and P.S. Hall. On-body diversity and angle-of-arrival measurement using a pattern switching antenna. Antennas and Propagation, IEEE Transactions on, 57(4):964–971, 2009. doi:10.1109/TAP.2009.2014597.
11. Yuan Shen and M.Z. Win. On the accuracy of localization systems using wideband antenna arrays. Communications, IEEE Transactions on, 58(1):270–280, 2010. doi:10.1109/TCOMM.2010.01.080141.
12. K.A. Gotsis, K. Siakavara, and J.N. Sahalos. On the direction of arrival (doa) estimation for a switched-beam antenna system using neural networks. Antennas and Propagation, IEEE Transactions on, 57(5):1399–1411, May 2009. doi:10.1109/TAP.2009.2016721.
13. R. M. Buehrer) Seyed A. (Reza, editor. Handbook of Position Localization Theory, Practice, and Advances. Wiley, 1 edition, 2012.
14. Nanyan Wang, P. Agathoklis, and A. Antoniou. A new doa estimation technique based on subarray beamforming. Signal Processing, IEEE Transactions on, 54(9):3279–3290, Sept 2006. doi:10.1109/TSP.2006.877653.
15. Qiaowei Yuan, Qiang Chen, and K. Sawaya. Accurate doa estimation using array antenna with arbitrary geometry. Antennas and Propagation, IEEE Transactions on, 53(4):1352–1357, April 2005. doi:10.1109/TAP.2005.844409.
16. Y. Takahashi, H. Yamada, and Y. Yamaguchi. Array calibration techniques for doa estimation with

arbitrary array using root-music algorithm. In Microwave Workshop Series on Innovative Wireless Power Transmission: Technologies, Systems, and Applications (IMWS), 2011 IEEE MTT-S International, pages 235–238, May 2011. doi:10.1109/IMWS.2011.5877119.
17. Xin Chen, Yu. Morton, and F. Dovis. A computationally efficient iterative mle for gps aoa estimation. Aerospace and Electronic Systems, IEEE Transactions on, 49(4):2707–2716, OCTOBER 2013. doi:10.1109/TAES.2013.6621847.
18. R.L. Johnson and G.E. Miner. An operational system implementation of the espirit df algorithm. Aerospace and Electronic Systems, IEEE Transactions on, 27(1):159–166, Jan 1991. doi:10.1109/7.68159.
19. B.N. Hood and P. Barooah. Estimating doa from radio-frequency rssi measurements using an actuated reflector. Sensors Journal, IEEE, 11(2):413–417, 2011. doi:10.1109/JSEN.2010.2070872.
20. Guangjie Han, Deokjai Choi, andWontaek Lim. Reference node placement and selection algorithm based on trilateration for indoor sensor networks. In Wireless Communications and Mobile Computing, Wirel. Commun. Mob. Comput. 2009; 9, pages 1017-1027, 2008. doi:10.1002/wcm.651.
21. J. Graefenstein, A. Albert, P. Biber, and A. Schilling. Wireless node localization based on rssi using a rotating antenna on a mobile robot. In Positioning, Navigation and Communication, 2009. WPNC 2009. 6th Workshop on, pages 253–259, 2009. doi:10.1109/WPNC.2009.4907835.
22. Abderrahim Benslimane, Clement Saad, Jean-Claude Konig, and Mohammed Boulmalf. Cooperative localization techniques for wireless ssensor networks: free, signal and anglebased techniques. In Wireless Communications and Mobile Computing, Wirel. Commun. Mob. Comput. 2014; 14, pages 1627-1646, 2012. doi:10.1002/wcm.2303.
23. R. Dean Straw. The ARRL Antenna Book. The national association for ARRL amateur radio, 21 edition, 2007.
24. C. A. Balanis. Antenna Theory, Analysis and Design. Wiley, 3 edition, 2005.
25. Ansys hfss. http://www.ansys.com/
26. M. Malajner, D. Gleich, and P. Planinsic. Angle of arrival measurement using multiple static monopole antennas. Sensors Journal, IEEE, 2015. doi:10.1109/JSEN.2014.2386537.
27. Mrf24j40ma - rf. http://www.microchip.com/
28. Interpolation - wikipedia, the free encyclopedia.
29. Curve fitting toolbox - matlab. http://www.mathworks.com/products/curvefitting/

Arrived: 09. 07. 2015
Accepted: 31. 12. 2015